Electronic supplementary information (ESI)

Alkylamine screening and zinc doping of highly luminescence 2D tin-halide perovskites for LED lighting

Yao Liu,‡[a] Aifei Wang,‡[b] Jiajing Wu,[a] Chuying Wang,[a] Ziliang, Li,[c] Guangcai Hu,[a] Shiqi Sui,[a] Jia-Xin She,[d] Wen Meng,[a] Weiqiang Li[d] and Zhengtao Deng*[a]

[a]*College of Engineering and Applied Sciences, State Key Laboratory of Analytical Chemistry for Life Science, National Laboratory of Microstructures, Nanjing University, Nanjing, Jiangsu, 210023, P. R. China. Email: dengz@nju.edu.cn;*

[b]*current address: Institute of Advanced Materials (IAM), Nanjing Tech University (NJ Tech), 5 Xinmofan Road, Nanjing 210009, P.R. China;*

[c]*Department of Electrical and Computer Engineering, University of Toronto, 10 King's College Road, Toronto, Ontario M5S 3G4, Canada;*

[d]*State Key Laboratory for Mineral Deposits Research, School of Earth Sciences and Engineering, Nanjing University, Nanjing, Jiangsu, 210023, PR China.*

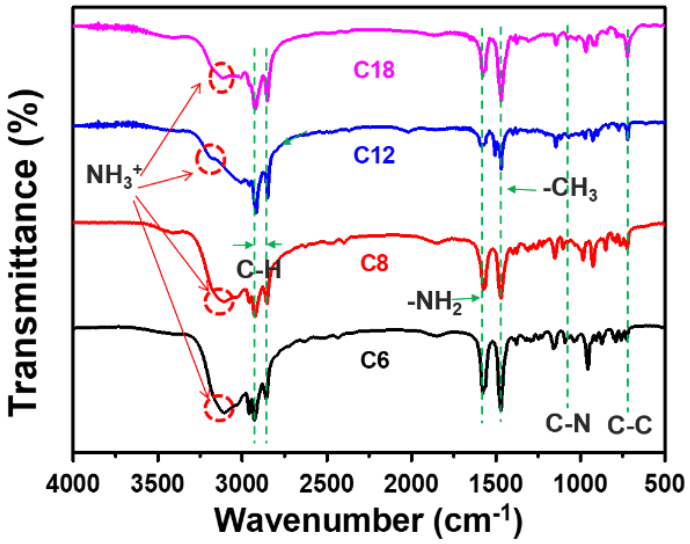

Fig. S1 FTIR spectra of 2D $(RNH_3)_2SnBr_4$ perovskites (For simplicity, we use C*n* to present $(RNH_3)_2SnBr_4$ samples and *n* stands for the number of carbon chain).

Some of the characteristic peaks of 2D $(RNH_3)_2SnBr_4$ perovskites are described as follows:

NH_3^+ stretching vibrations: ~3108 cm^{-1} (C6), ~3110 cm^{-1}(C8),

~3193 cm^{-1} (C12), ~3118 cm^{-1} (C18)

-NH_2 bending vibrations: ~1570 cm^{-1}

C-H symmetric and asymmetric stretching vibrations: ~2850 cm^{-1} and ~2920 cm^{-1}

-CH_3 bending vibrations: ~1470 cm^{-1}

C-N stretching vibrations: ~1071 cm^{-1}

C-C stretching vibrations: ~722 cm^{-1}

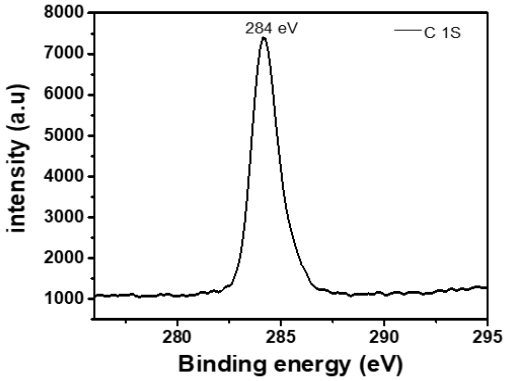

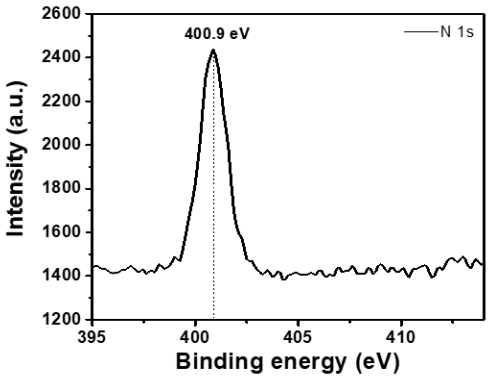

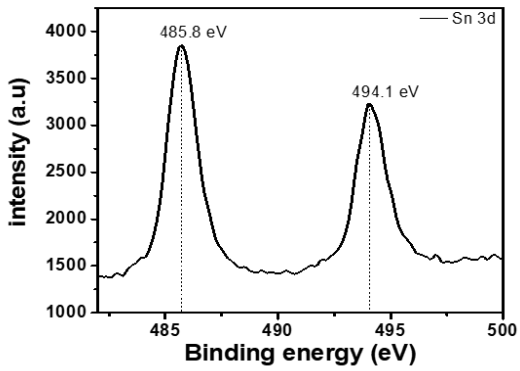

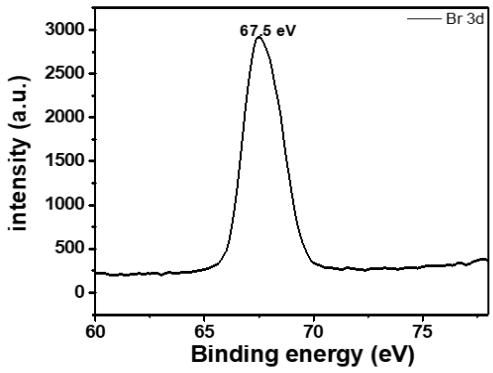

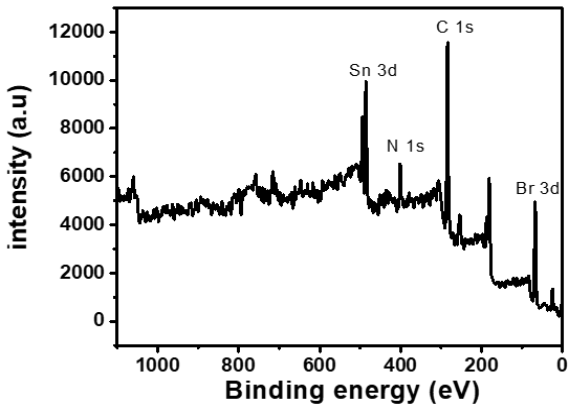

Fig. S2 High-resolution XPS spectra of C, N, Sn, and Br elements of 2D $(C_8H_{17}NH_3)_2SnBr_4$ perovskites.

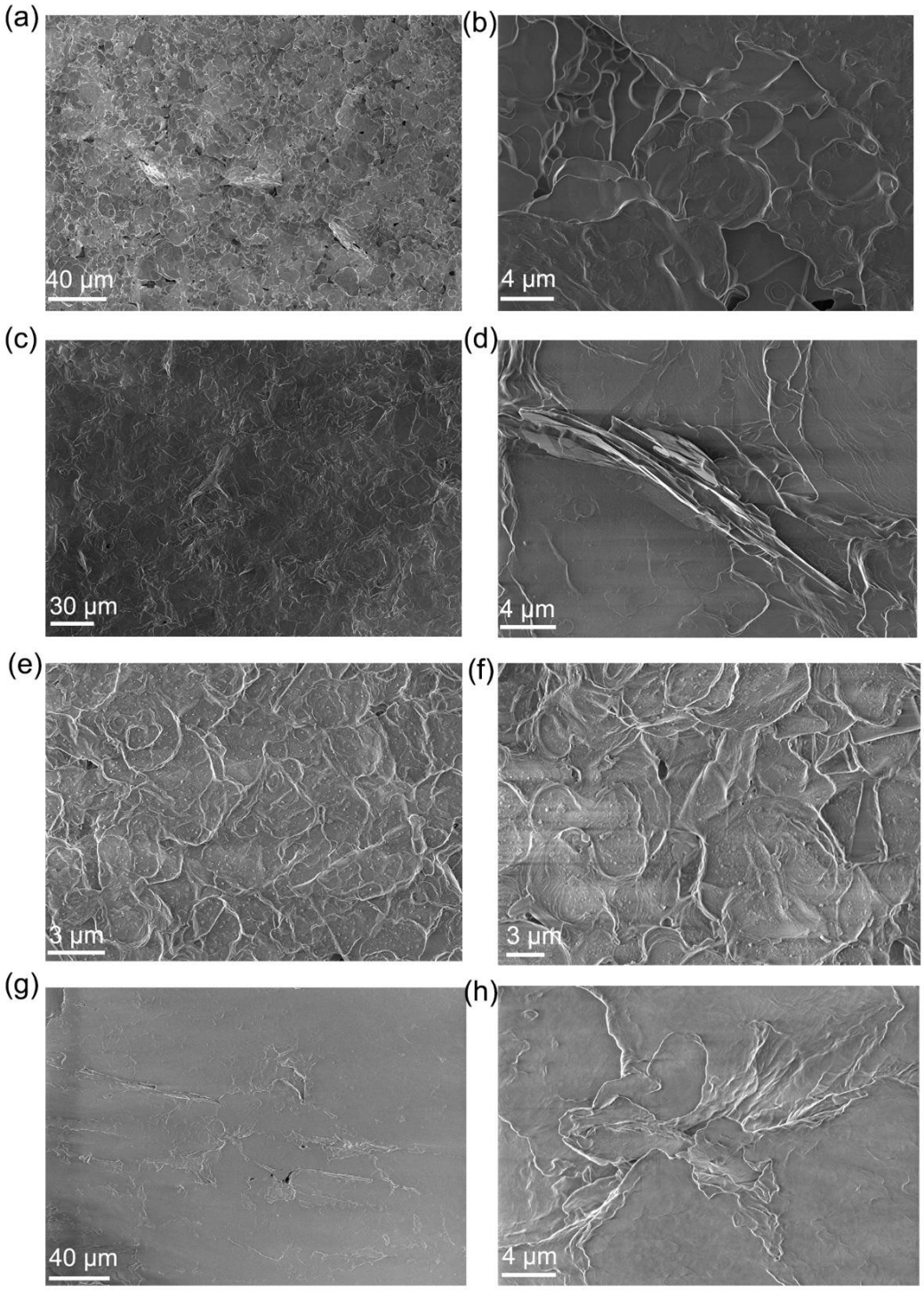

Fig. S3 Scanning electron microscopy (SEM) images of $(C_6H_{13}NH_3)_2SnBr_4$ (a, b), $(C_8H_{17}NH_3)_2SnBr_4$ (c, d), $(C_{12}H_{25}NH_3)_2SnBr_4$ (e, f), and $(C_{18}H_{35}NH_3)_2SnBr_4$ (g, h) perovskites at other magnifications.

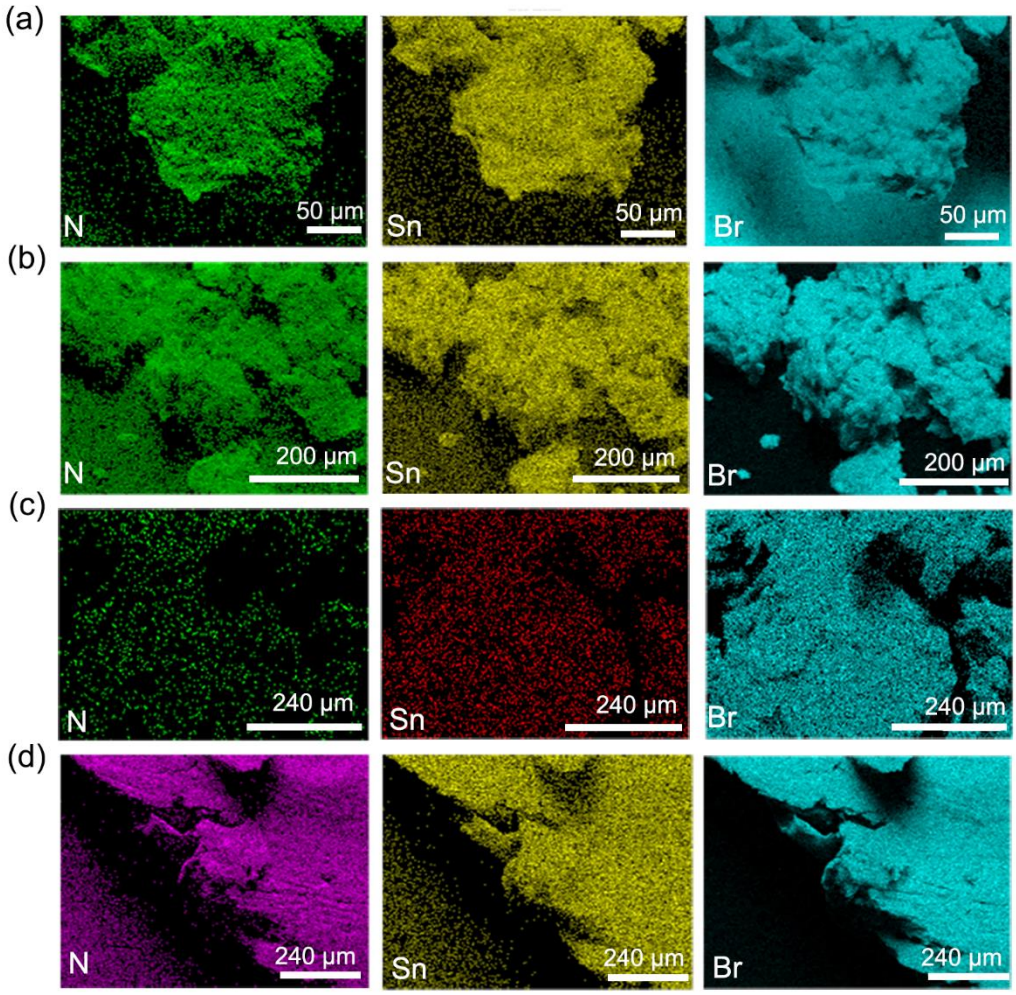

Fig. S4 Energy-dispersive X-ray spectroscopy (EDS) mapping images of $(C_6H_{13}NH_3)_2SnBr_4$ (a), $(C_8H_{17}NH_3)_2SnBr_4$ (b), $(C_{12}H_{25}NH_3)_2SnBr_4$ (c), and $(C_{18}H_{35}NH_3)_2SnBr_4$ (d) perovskites.

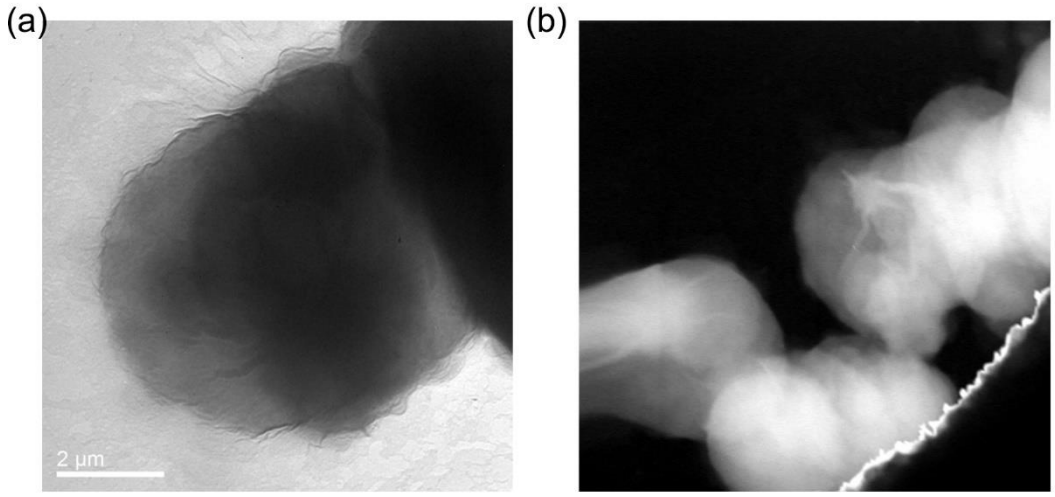

Fig. S5 TEM (a) and HAADF-STEM (b) images of $(C_{18}H_{35}NH_3)_2SnBr_4$ perovskites.

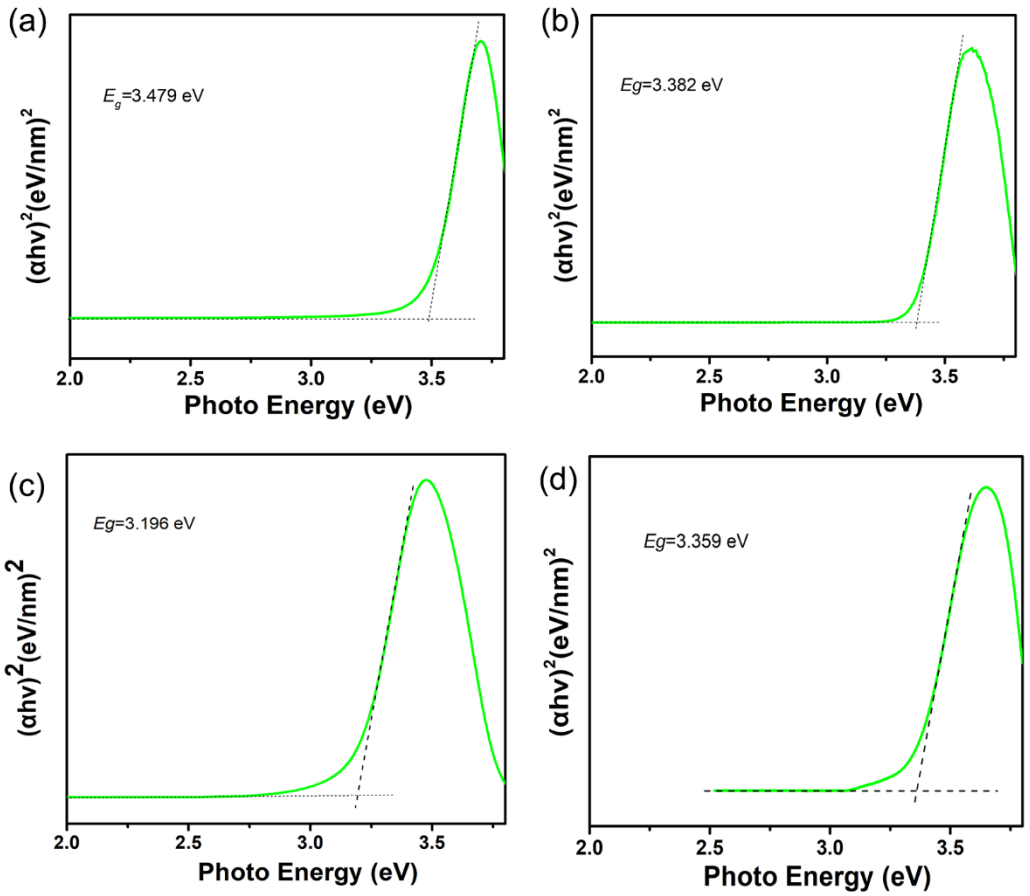

Fig. S6 Plots of $(\alpha hu)^2$ *vs* photo energy (hu) of 2D $(C_6H_{13}NH_3)_2SnBr_4$ (a), $(C_8H_{17}NH_3)_2SnBr_4$ (b), $(C_{12}H_{25}NH_3)_2SnBr_4$ (c), and $(C_{18}H_{35}NH_3)_2SnBr_4$ (d) perovskites.

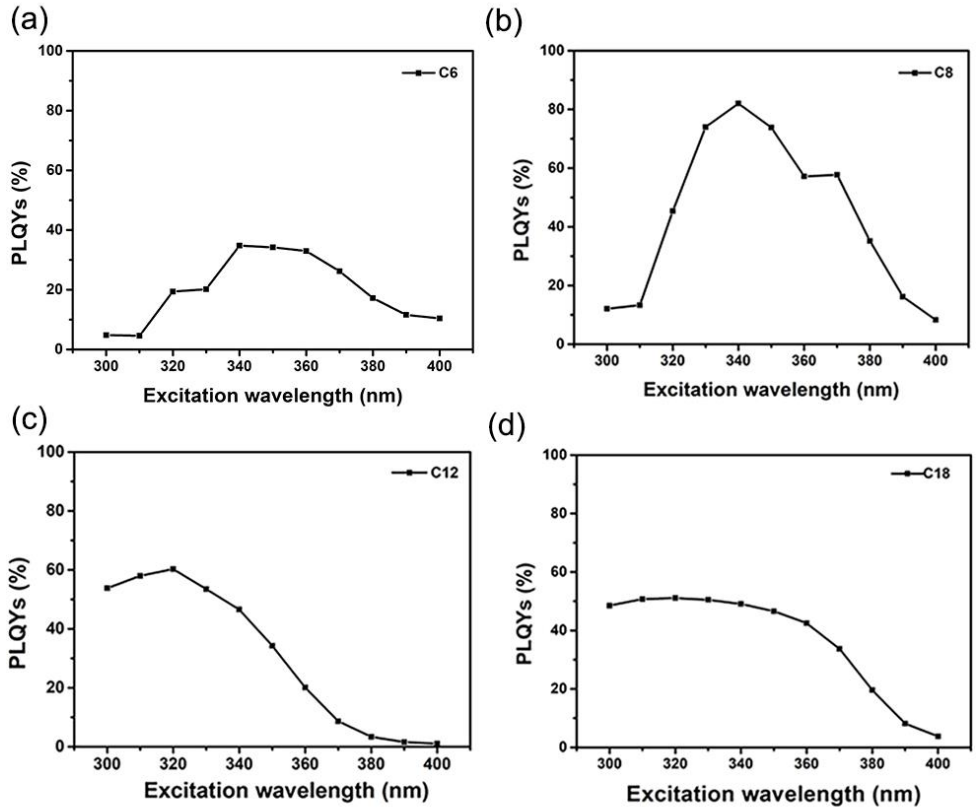

Fig. S7 (a, b, c, d) The absolute PLQYs of as-synthesized 2D $(RNH_3)_2SnBr_4$ perovskites under different excitation wavelengths. (For simplicity, we use C*n* to present $(RNH_3)_2SnBr_4$ samples and *n* stands for the number of carbon chain).

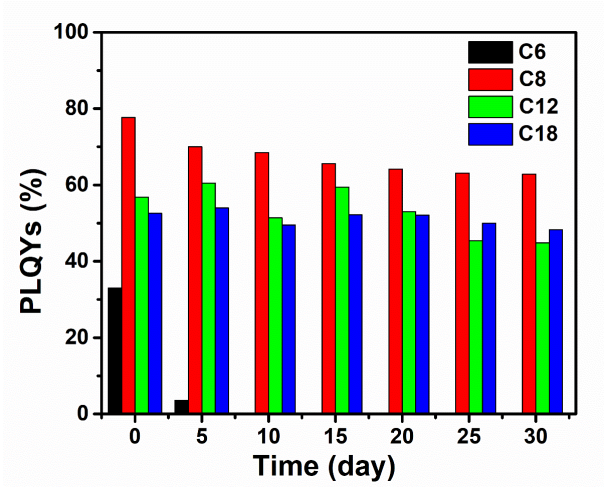

Fig. S8 Stability curves displayed by the PLQYs of $(RNH_3)_2SnBr_4$ perovskites. (For simplicity, we use C*n* to present $(RNH_3)_2SnBr_4$ samples and *n* stands for the number of carbon chain).

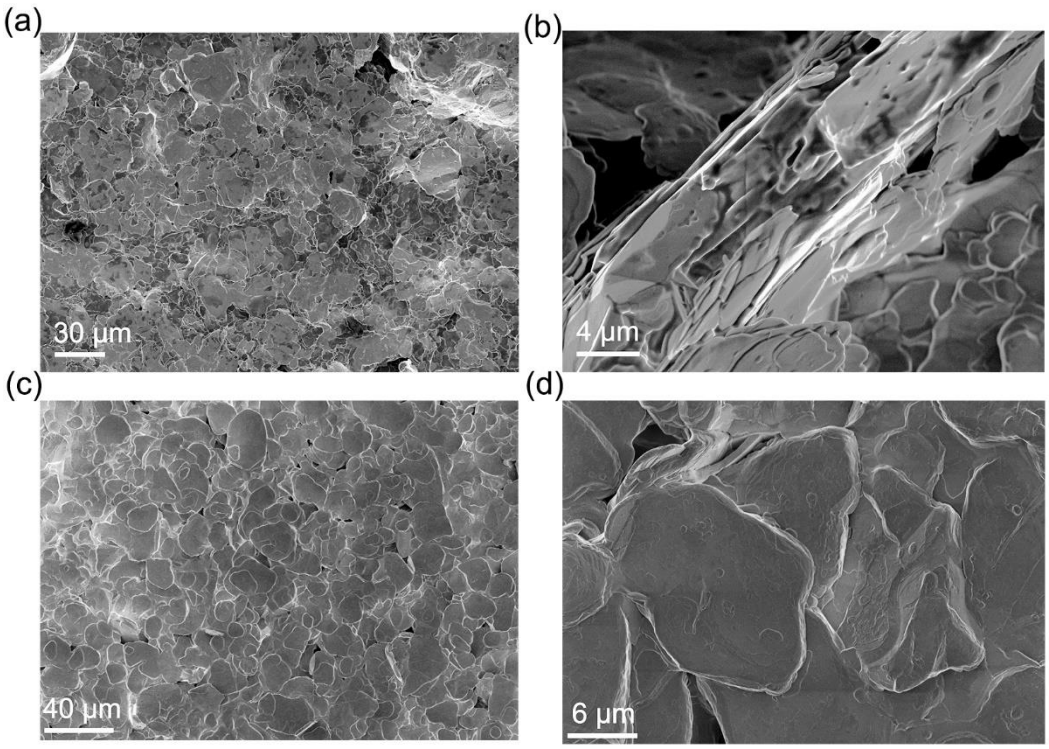

Fig. S9 Other scanning electron microscopy (SEM) images of 2D $(C_8H_{17}NH_3)_2Sn(2Br/I)_4$ (a, b) and $(C_8H_{17}NH_3)_2SnI_4$ (c, d) perovskites at different magnifications.

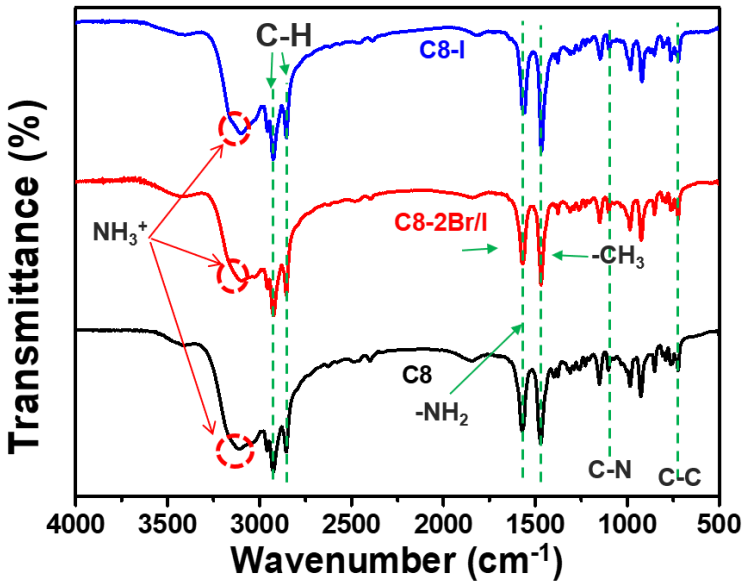

Fig. S10 FTIR spectra of 2D $(C_8H_{17}NH_3)_2Sn(2Br/I)_4$ and $(C_8H_{17}NH_3)_2SnI_4$ perovskites.

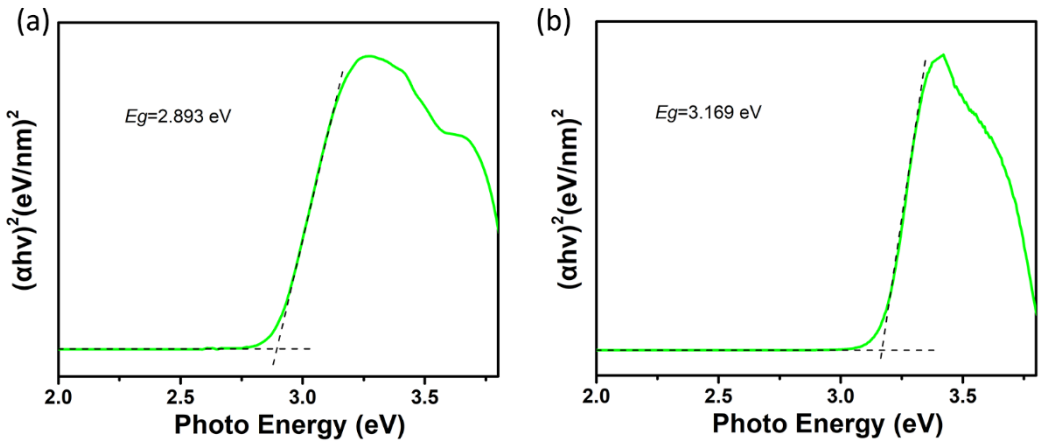

Fig. S11 Plots of $(\alpha h\upsilon)^2$ *vs* photo energy ($h\upsilon$) of $(C_8H_{17}NH_3)_2Sn(2Br/I)_4$ (a) and $(C_8H_{17}NH_3)_2SnI_4$ (b) perovskites.

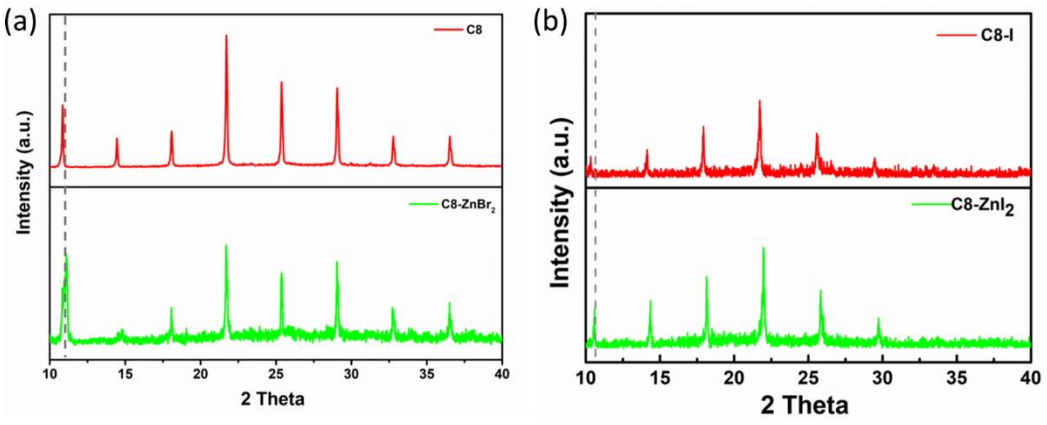

Fig. S12 Powder X-ray diffraction (PXRD) patterns for Zn^{2+}-doped and undoped $(C_8H_{17}NH_3)_2SnBr_4$ (a), Zn^{2+}-doped and undoped $(C_8H_{17}NH_3)_2SnI_4$ perovskites (b).

Table. S1 Radiative transition rate (k_r), non-radiative transition rate (k_{nr}) and k_r / k_{nr} of the samples.

Sample	PLQY (%)	τ_{avg} (μs)	k_r (μs^{-1})	k_{nr} (μs^{-1})	kr/ k_{nr}
$(C_6H_{13}NH_3)_2SnBr_4$	35.0	1.60	0.2188	0.4063	0.5385
$(C_8H_{17}NH_3)_2SnBr_4$	82.0	4.99	0.1643	0.0361	4.5550
$(C_{12}H_{25}NH_3)_2SnBr_4$	60.2	5.31	0.1136	0.0750	1.5150
$(C_{18}H_{35}NH_3)_2SnBr_4$	50.5	5.21	0.0988	0.0931	1.0612

Table. S2 τ_{avg} and R^2 of the undoped and doped samples.

	C8	C8-$ZnBr_2$	C8-I	C8-ZnI_2
τ_{avg} (μs)	4.99	4.40	1.41	1.93
R^2	0.999	0.999	0.998	0.995

Table. S3 Radiative transition rate (k_r), non-radiative transition rate (k_{nr}) and k_r/k_{nr} of the samples.

Sample	PLQY (%)	τ_{avg} (μs)	k_r (μs^{-1})	k_{nr} (μs^{-1})	k_r/k_{nr}
C8	82.0	4.99	0.1643	0.0361	4.5550
C8-$ZnBr_2$	85.0	4.40	0.1932	0.0341	5.6670
C8-I	33.0	1.51	0.2340	0.4752	0.4924
C8-ZnI_2	50.0	1.93	0.2591	0.2591	1.0000